

MMIC Package Characterization with Active Loads¹

Kurt Phillips
Dylan Williams

National Institute of Standards and Technology
325 Broadway
Boulder, Colorado
80303

Abstract

A technique for characterizing microwave packages based on active PIN diode standards is discussed. The technique allows packages to be accurately characterized from external reflection coefficient measurements when a single bias-dependent active standard is embedded within it. The frequency characteristics, stability, and linearity of active PIN diode standards are investigated.

Introduction

In this paper we will discuss a technique for characterizing packages electrically at microwave frequencies using active loads. This technique is useful because packaging may significantly affect the electrical characteristics of a microwave circuit. This is particularly true with monolithic microwave integrated circuit (MMIC) packaging, since electrical performance must often be balanced against physical constraints and limitations associated with fabrication and device insertion methods.

We will assume in this paper that the package transitions can be represented electrically as two-ports. A number of schemes are available to de-embed such transitions. If the package itself has exactly two transitions, it may be amenable to a two-tier TRL (Thru-Reflect-Line) de-embedding,¹ which accurately determines the scattering parameters (S-parameters) of both transitions. TRL, however, requires the insertion of lines of two different lengths. This is prohibited by fixed package dimensions. Although the longer line may be meandered to shorten its port-to-port length, reflections at the bends degrade the accuracy of the standard. Thus TRL is limited to two-port packages without fixed port-to-port spacing.

For two-port packages and fixtures of fixed dimension, a

¹ Publication of the National Institute of Standards and Technology, not subject to copyright. This work was sponsored in part by the Naval Air Systems Command under contract N00019-89-C-0150 and by the NIST Consortium for MIMIC Metrology.

technique commonly applied utilizes only a single transmission line as a standard.² Since measurement of this line does not provide enough information to characterize the package transitions, complicated models intended to represent the package must be developed. The accuracy of these models is often difficult to ascertain.

Both of these techniques are applicable only to two-port packages and require line standards whose length is customized to the package. A more nearly universal method relies solely on one-port reflective standards. Assuming reciprocal transitions, a minimum of three one-port standards is required; a short, an open, and a load are the typical choices. In many cases, however, the standards need to be soldered or epoxied into the package. This makes insertion difficult and the use of multiple standards impractical.

A characterization method based upon a single active device at different bias states offers the opportunity to use, in effect, multiple standards with only a single insertion and without fixing the port-to-port distance. In such a scheme, we model the package as a linear two-port transition attached to each port of the circuit. The reflection coefficients of the active device at different DC biases are determined by measurements performed before the insertion of the standard into the package. After insertion, the reflection coefficients of the package with the known, embedded one-port standard are measured at the same set of biases. This allows the S-parameters of the two-port which characterizes the package transition to be deduced by standard de-embedding techniques such as that described by Bauer and Penfield.³

In this paper we will discuss such a scheme for accurately characterizing the microwave transitions of microwave circuits using active PIN diode standards. The scheme is intended for use in a wide variety of packages with different port-to-port distances and insertion techniques, some of which may require that the standard be temperature cycled during insertion into the package. We will show that beam lead PIN diodes have the required stability, repeatability, and frequency response for use in this type of application up to 40 GHz. We will also determine the linear operating range of the diodes and demonstrate the de-embedding procedure.

Diode Properties

We chose to investigate three silicon PIN diodes and one gallium arsenide PIN diode supplied by different manufacturers for use as active standards. We fabricated a Thru-Reflect-Line (TRL) calibration set in coplanar waveguide (CPW) in order to electrically characterize the diodes on our microwave wafer probe station. The calibration set consisted of two CPW lines of length 11.6 mm and 3.6 mm, a 1.6 mm CPW thru line, and a pair of 0.8 mm offset shorts. The calibration set was fabricated by etching a thin gold film off of a pre-coated alumina substrate. The CPW

center conductor was 150 μm wide and the gaps between the two outer ground planes and the center conductor were 65 μm wide. These dimensions were selected so that the guide would have a nominal impedance of 50 Ω and so that the center conductor would be wide enough to easily accommodate the leads of the PIN diodes. For testing, the diodes were embedded in the circuit depicted in Figure 1.

We performed a TRL calibration and measured the reflection coefficient of the PIN diodes with respect to the reference plane shown in Figure 1. An example, plotted on the Smith chart in Figure 2, shows that, at a hard forward bias of 1.03 V and 6.78 mA, a reverse bias of -6 V, and an intermediate forward bias of 0.7 V and 0.015 mA, the reflection coefficients of the diode remain widely separated on the chart up to 40 GHz. This is a prerequisite to accurate de-embedding.³

We developed the simple model circuit shown in Figure 3 in order to analyze the frequency dependence of the measured reflection coefficient. The two leads of the beam lead diodes were of approximately the same width as the CPW center conductor, so we modeled them as short sections of CPW. The lengths of these sections were chosen to correspond to the physical length of the mount. The CPW short was modeled as a 0.035 nH inductor, whose value was determined in a separate experiment. The intrinsic diode was modeled by a series junction resistance of 4 Ω , a shunt junction capacitance of 0.022 pF, and a bias-dependent shunt junction resistance R_d . These values were chosen so as to create a good fit between the modeled and measured reflection coefficients. The values of R_d were 0 Ω , 47.5 Ω , and ∞ when the diode was forward, intermediate, and reverse biased, respectively.

The fit between the measured and modeled reflection coefficient of the diode was quite good except for the intermediate resistive state at very low frequencies. Charge storage effects, which are not accounted for in the model, may account for the discrepancy. We used the model to extrapolate the performance of the diodes to higher frequencies, as shown in Figure 2. The model predicts that the three bias states will remain widely separated on the Smith chart until about 80 GHz. This indicates that this diode and mount (the best we tested) could probably be used for de-embedding to 80 GHz. Above 80 GHz, the model predicts that the bias states rapidly approach each other as the frequency increases, so the diode is unsuitable for de-embedding.

The de-embedding procedure will fail if the reflection coefficient of the diode and its mount changes upon being soldered into the package. We performed an experiment to test for the stability of the PIN diodes with respect to temperature cycling. We began the experiment by measuring the reflection coefficients of each of the diodes when forward biased, unbiased, and biased to an intermediate resistive state. We then remeasured the reflection coefficients and calculated the absolute value of the difference from the first measurement; representative results at 40 GHz are

tabulated in the first row of Table 1.

After performing this control measurement, we temperature-cycled the PIN diodes twice. We were unable to determine the exact time-temperature profiles with our experimental setup, but estimated that a peak temperature of 300°C was maintained for a minute or two during the first temperature cycle and that a peak temperature of 290°C was maintained for about 20 minutes during the second temperature cycle. After each temperature cycle we remeasured the reflection coefficients of the diodes and again calculated the absolute value of the difference between the first and the subsequent measurements. The results are tabulated in the second and third rows of Table 1. From Table 1 we see that all of the diodes we tested exhibited excellent stability.

An important criterion for an active standard is linearity. If the power at which the reflection coefficient is measured is too high, the microwave impedance of the diode will shift as the incident power changes, so the de-embedding procedure will fail. We performed calibrations and measurements of the reflection coefficients of the diodes at several incident powers. We found that the reflection coefficient of the diodes deviated from its extrapolated small-signal value by less than 0.1% when the incident power was increased to -30 dBm. Our ANA can only withstand only a small decrease from its maximum signal power before the accuracy of the measurement starts to deteriorate, but a reduction in incident power can be compensated for by an increase in the IF averaging factor. At -30 dBm, the number of points in the IF average had to be increased to 1000 per frequency to obtain measurement accuracy comparable to that of the ANA when operated at its nominal signal of approximately 0 dBm.

Finally, the possibility that errors could be introduced by light incident upon the diode was investigated. An estimated 730 mW/cm² of white light from the microscope incident on the wafer changed the magnitude of the reflection coefficient of the diode by only 2.3×10^{-5} . This change is negligible and suggests that typical lighting will not affect the diode impedance significantly.

Experimental Verification of the De-embedding Procedure

The de-embedding procedure was verified with diode #3, using the probe heads as the transitions to be measured, as illustrated in Figure 4. We set the IF averaging factor to 1000 and the incident power to just below -30 dBm. We first measured the reflection coefficient of diode #3 when forward biased, reverse biased, and biased in three different intermediate resistive states with respect to an on-wafer CPW TRL calibration. We then measured the reflection coefficients of the probe head/diode combination, in the same five bias states, with respect to the calibration we had performed earlier at the probe head coaxial connection.

After these measurements, we applied the de-embedding algorithm developed by Bauer and Penfield³ to determine the S-

parameters of the probe heads from the two sets of measurements. This algorithm uses a least-squares fit to the redundant measurements. To verify the result, we repeated the experiment using a two-tier TRL calibration instead. The same procedure was used except that a TRL standard set was substituted for the characterized diodes and a TRL algorithm¹ was used to de-embed the S-parameters of the probe head. The results are plotted in Figure 5 and the agreement is excellent.

Conclusion

PIN diodes are suitable as active standards for characterizing microwave transitions. The bias-dependent de-embedding scheme requires only a single insertion of a one-port standard at each port and is therefore particularly well suited to the characterization of microwave packages. The de-embedding scheme was demonstrated over the frequency range of 50 MHz to 40 GHz and shows promise for use at frequencies as high as 80 GHz.

References

1. R. Marks and K. Phillips, "Wafer-level ANA calibrations at NIST," 34th ARFTG Conference Digest, 1989.
2. P. B. Ross and B. D. Geller, "A broadband microwave test fixture," Microwave Journal, vol. 30, no. 5, May 1987, pp. 233-248.
3. R. F. Bauer and P. Penfield, "De-embedding and unterminating," IEEE Transactions on Microwave Theory and Tech., vol. MTT-22, no. 3, pp. 282-288, March 1974.

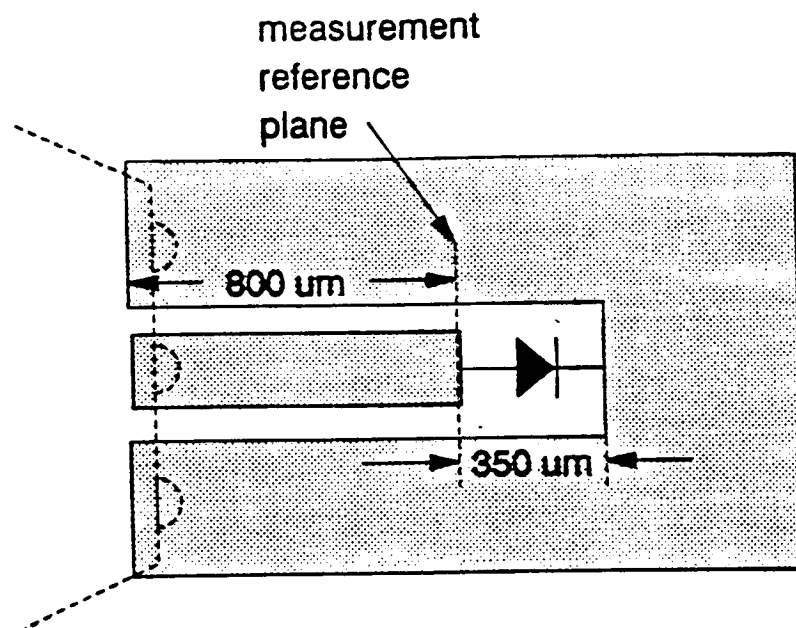
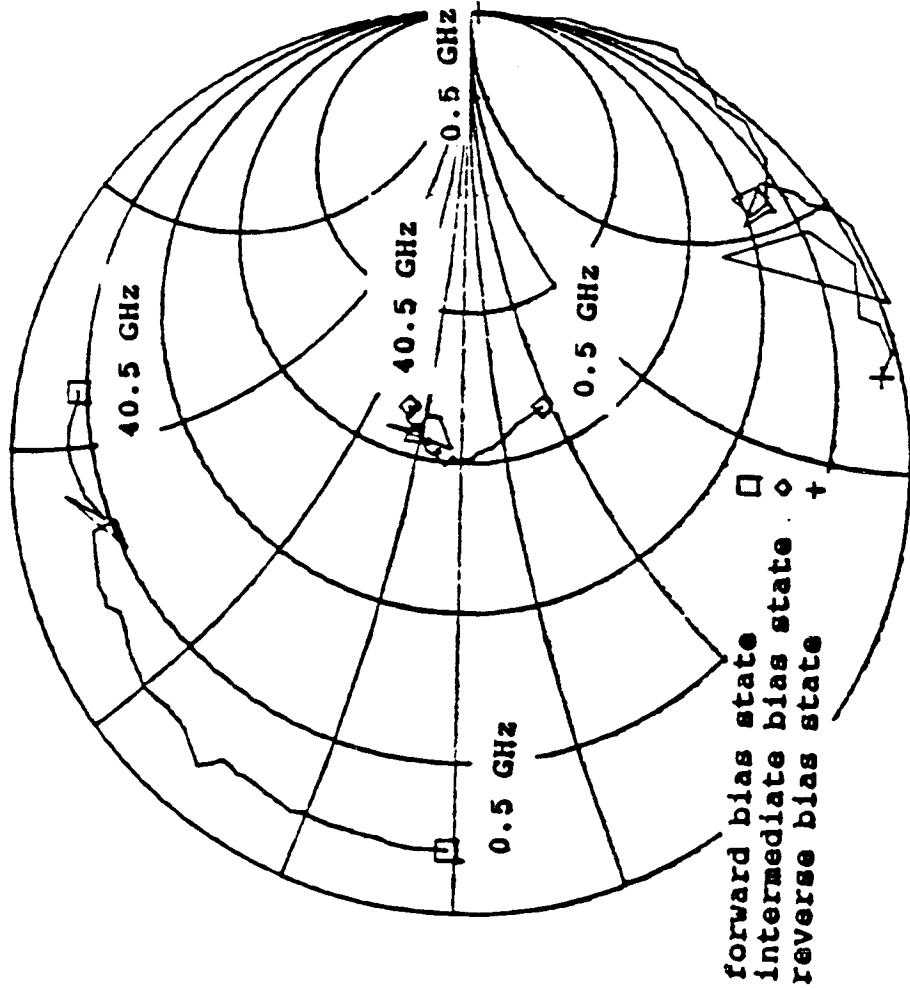


Figure 1. The diode test structure and mount. The probe tip placement and measurement reference plane are shown.

	Bias State	Diode #1	Diode #2	Diode #3	Diode #4
CONTROL	Forward	0.017	0.008	0.002	0.004
	Resistive	0.002	0.003	0.004	0.004
	No Bias	0.002	0.015	0.006	0.002
After 300°C temp. cycle	Forward	0.028	0.027	0.003	0.023
	Resistive	0.015	0.013	0.006	0.021
	No Bias	0.012	0.037	0.010	0.013
After 290°C temp. cycle	Forward	0.058	0.029	0.022	0.027
	Resistive	0.013	0.012	0.022	0.025
	No Bias	0.013	0.033	0.030	0.015

Table 1. The absolute change in each diode's reflection coefficient for the three bias states caused by temperature cycling are tabulated. The control measurement was used to characterize the measurement error. All of the diodes were silicon PIN diodes except diode #1, which was fabricated on gallium arsenide.

MEASURED



forward bias state
intermediate bias state
reverse bias state

MODELED

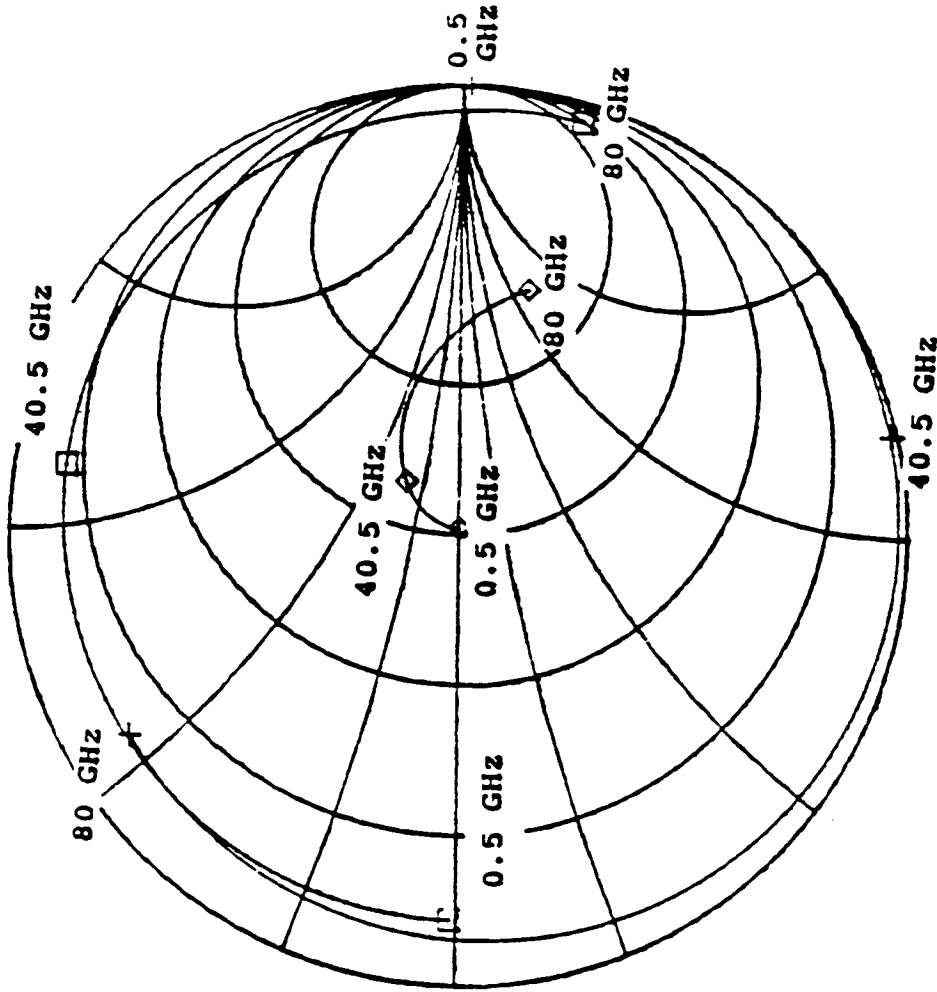


Figure 2. The measured and modeled reflection coefficients when diode #3 was reversed biased, biased to an intermediate resistive state, and forward biased are shown.

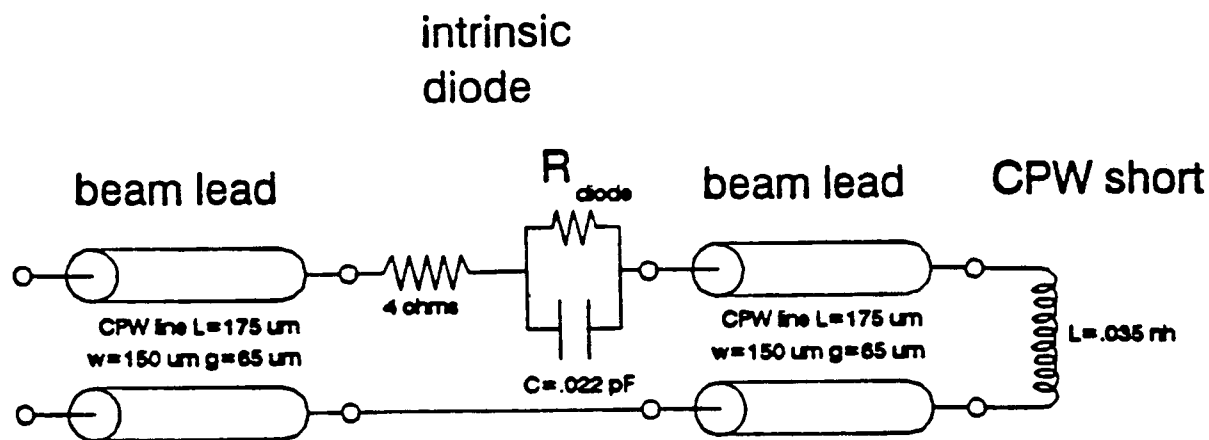


Figure 3. The equivalent circuit used to model the measured diode reflection coefficient and to extrapolate the performance of the diode and mount to higher frequencies is shown.

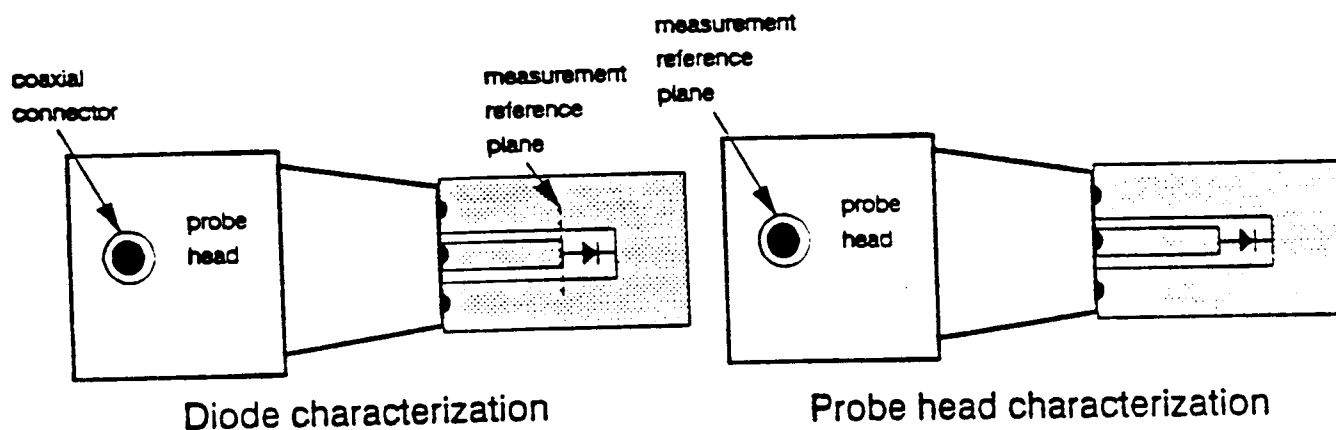


Figure 4. The procedure used to characterize the probe head with the active PIN diode standards is illustrated. First the reflection coefficient of the diodes in various bias states was measured with respect to an on-wafer TRL calibration. Then the reflection coefficient of the probe head and diode at the same bias states was measured with respect to a coaxial calibration at the probe head connector. The information from these measurements is sufficient to determine the S-parameters of the probe head. The same technique can be applied to package characterization.

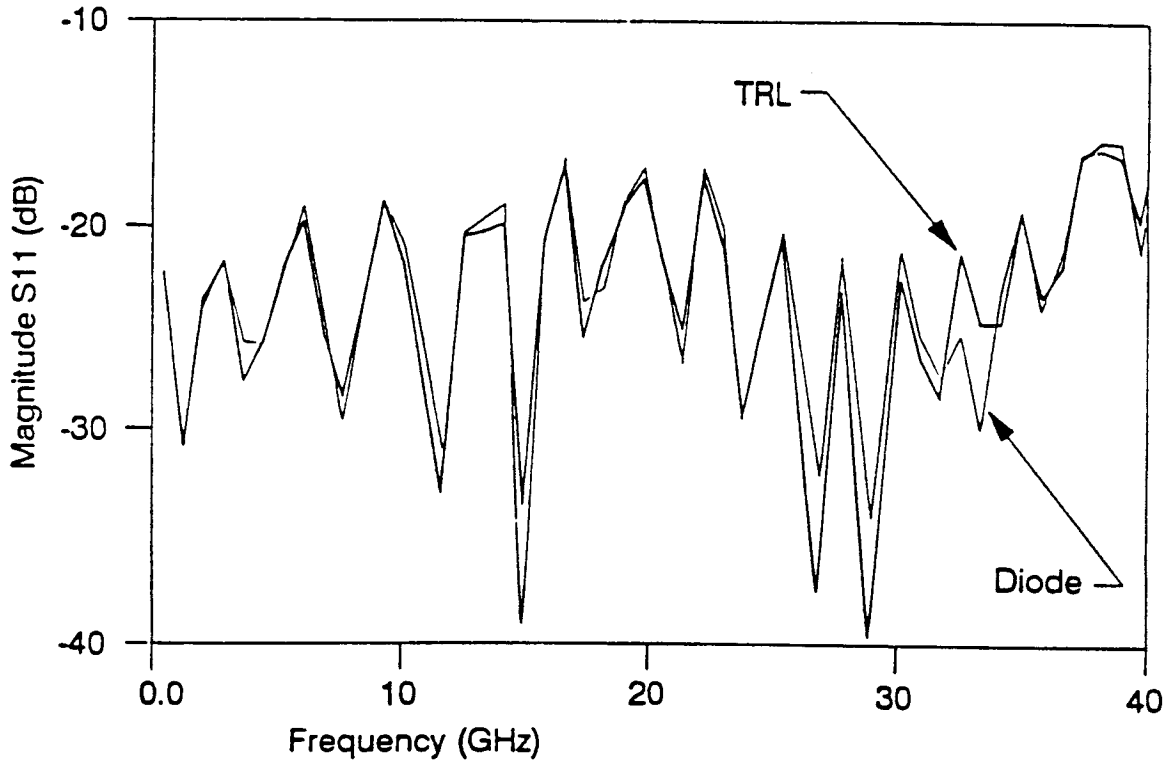
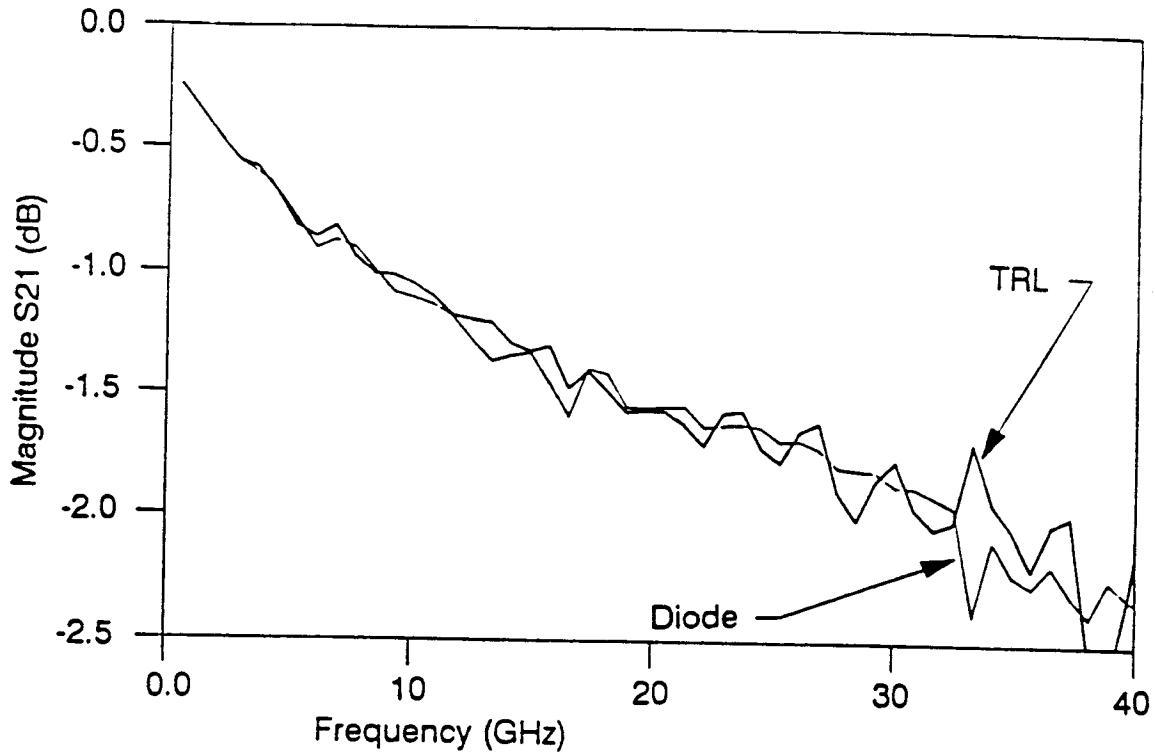


Figure 5. The S-parameters of the probe head determined by de-embedding using the active standards and using the TRL standards are compared.